A DOA and polarization estimation method using a spatially non-collocated vector sensor array

Conference Paper · July 2014

DOI: 10.1109/ChinaSIP.2014.6889347

4 authors, including:

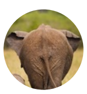

Yikai Wang
University of Electronic Science and Technology of China

A DOA AND POLARIZATION ESTIMATION METHOD USING A SPATIALLY NON-COLLOCATED VECTOR SENSOR ARRAY

Fang Liu, Huiyong Li†, Wei Xia†, and Yikai Wang

School of Electronic Engineering, University of Electronic Science and Technology of China
Chengdu, 611731

ABSTRACT

To reduce the mutual coupling across the collocated sensor, a distributed array geometry composed of crossed dipole pair is introduced in this paper. Based on the non-collocated vector sensor array, an ESPRIT-based method is newly proposed to estimate the direction of arrival (DOA) and polarization parameter. Due to the special structure of non-collocated array, the DOA and polarization parameter are paired automatically, and thus the computational complexity is greatly reduced. The Cramer-Rao Lower Bound (CRLB) has been derived and the performance of DOA and polarization estimation for the distributed array is also analyzed. Simulation results verify the effective parameter estimation performance of the proposed method by using a spatially non-collocated array.

***Index Terms*—**mutual coupling, DOA, polarization estimation, non-collocated vector sensor array, CRLB

1. INTRODUCTION

Electromagnetic vector sensor array can utilize both the spatial and polarization information of impinging wave-fields, so it can achieve a better performance of parameter estimation and beamforming than the conventional scalar sensor array [1-2]. In the past few decades, vector sensor array has attracted much attention and many array processing techniques using vector sensors have been developed [3-7]. However, in the previous study, the electromagnetic vector sensor is usually assumed to be configured by 2 to 6 collocated orthogonal magnetic loops and electric dipoles. The collocated array is easily subjected to mutual coupling across these collocated components. Also the mutual coupling will degrade the performance of vector sensor, increase the hardware cost of antenna implementation and the multiple components leads to a huge computational burden [8].

As mutual coupling is unavoidable, spatially distributed electromagnetic component sensor array has been proposed to alleviate the mutual coupling [9]. By spatially distributing a complete electromagnetic vector sensor, the modified vector-cross-product direction finding algorithm is proposed to estimate the DOA and polarization parameter in [10]. The CRLB of the distributed array composed of a complete electromagnetic vector sensor has been analyzed in [11]. However, the modified vector-cross-product algorithm is only applicable to a complete electromagnetic vector sensor which is composed of the whole 6 components. In practice, the response of electric field and magnetic field is varying different from each other, thus only dipoles or loops are a better choice to form a vector sensor array [12]. Then, the modified vector-cross-product direction finding algorithm is no longer suitable for the dipole triads or loop triads.

The filtering performance of the non-collocated crossed dipole pair is discussed in [13], but the parameter estimation method about the identical array form has not been reported. In this paper, a uniform linear array with non-collocated crossed dipole pair is introduced for DOA and polarization estimation. The non-collocated array contains only one dipole on every uniform array-grid and the mutual coupling is greatly reduced compared with the collocated array. A DOA and polarization estimation method is proposed based on the ESPRIT algorithm herein. Furthermore, the DOA and polarization parameter are paired automatically, thus the computational complexity is greatly reduced. Finally, simulation results demonstrate the validity of the proposed method.

The rest of this paper is organized as follows. The distributed array geometry is introduced and the signal model is given in section 2. The derivation of the proposed method is presented and the estimation expressions of parameters are shown in Section 3. The performance of the algorithm evaluated in computer simulations is described in section 4. Finally, section 5 presents the conclusion of this work.

This work was supported in part by the National Nature Science Foundation of China under Grants 61371184, 61301262 and 61101173.
Corresponding authors: Huiyong Li and Wei Xia.

2. SIGNAL MODEL

The two-component vector sensor array composed of $M/2$ collocated crossed dipole pair is shown in Fig.1 and M is even. By placing each component of crossed dipole pair alternately, the non-collocated array geometry composed of M spatially spread electric dipoles is shown in Fig.2. All the dipoles are arranged uniformly in the y-axis and deployed parallelled to x-axis and y-axis directions, respectively. The inter-element spacing is equal to d. To simplify the analysis, the incident signals are assumed to be completely polarized electromagnetic wave and the transmission medium is isotropic and homogeneous.

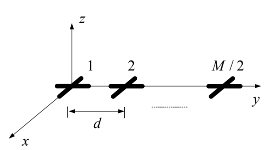

Fig.1 The collocated array geometry

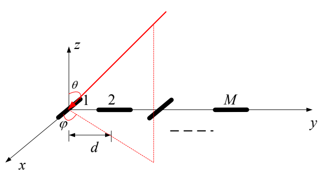

Fig.2 The non-collocated array geometry

The two-component polarization steering vector [4] of each collocated sensor in Fig.1 can be described as

$$\begin{bmatrix} p_x \\ p_y \end{bmatrix} = \begin{bmatrix} -\sin\varphi & \cos\theta\cos\varphi \\ \cos\varphi & \cos\theta\sin\varphi \end{bmatrix} \begin{bmatrix} \cos\gamma \\ \sin\gamma e^{j\eta} \end{bmatrix} \tag{1}$$

where p_x and p_y denote the polarization responses of electric dipoles parallelled to x-axis and y-axis respectively. $0 \le \gamma < \pi/2$ signifies the auxiliary polarization angle, and $-\pi \le \eta < \pi$ represents the polarization phase difference. $-\pi/2 \le \theta \le \pi/2$ and $0 \le \varphi < 2\pi$ denote the incident source's elevation angle and azimuth angle, respectively. Assume the azimuth angle of each incident signal to be $\varphi = \pi/2$, then equation (1) can be simplified as

$$\begin{bmatrix} p_x \\ p_y \end{bmatrix} = \begin{bmatrix} -\cos\gamma \\ \cos\theta\sin\gamma e^{j\eta} \end{bmatrix}. \tag{2}$$

As the same type of the electric dipoles has the identical polarization response to incident electromagnetic wave, then the $M \times 1$ polarization steering vector of the non-collocated array in Fig.2 is

$$\boldsymbol{a}_p = [p_x, p_y, p_x, \cdots, p_y]^{\mathrm{T}}. \tag{3}$$

Since the components of each sensor in Fig.1 are spatially spread in Fig.2, the space phase delay will be introduced between the adjacent elements. The space steering vector of the non-collocated array is

$$\boldsymbol{a}_s = \left[1, e^{j\phi}, \cdots, e^{j(M-1)\phi}\right]^{\mathrm{T}} \tag{4}$$

where j represents the imaginary unit of complex and $\phi = 2\pi d\sin\theta/\lambda$. The joint polarization-space steering vector of non-collocated array in Fig.2 can be described as Hadamard product of polarization steering vector and space steering vector, then the joint steering vector is

$$\boldsymbol{a} = \boldsymbol{a}_p \odot \boldsymbol{a}_s = \left[p_x, p_y e^{j\phi}, p_x e^{j2\phi}, \cdots, p_y e^{j(M-1)\phi}\right]^{\mathrm{T}} \tag{5}$$

where $\odot$ denotes the Hadamard product. Assume that there are K narrow-band signals impinging on the non-collocated array, the received signal vector $\boldsymbol{X}(t)$ is then

$$\boldsymbol{X}(t) = \left[x_1(t), x_2(t), \cdots, x_M(t)\right]^{\mathrm{T}} = \sum_{k=1}^{K} \boldsymbol{a}_k \cdot s_k(t) + \boldsymbol{N}(t) \tag{6}$$

where $s_k(t)$ denotes the complex envelope of the kth incident stochastic signal, $\boldsymbol{a}_k$ is the kth joint polarization-space steering vector, and $\boldsymbol{N}(t)$ represents the zero-mean, additive complex Gaussian noise.

3. ALGORITHM DERIVATION

The covariance matrix of the received signal has the form

$$\boldsymbol{R_X} = \mathrm{E}\left\{\boldsymbol{X}(t)\boldsymbol{X}(t)^{\mathrm{H}}\right\} = \boldsymbol{A}\boldsymbol{R_S}\boldsymbol{A}^{\mathrm{H}} + \sigma_{\mathrm{n}}^2 \boldsymbol{I}_M \tag{7}$$

where $\boldsymbol{R_S} = \mathrm{diag}([\sigma_1^2, \sigma_2^2, \cdots, \sigma_K^2])$ is the autocorrelation matrix of the incident signals $\boldsymbol{S}(t) = \mathrm{diag}([s_1(t), s_2(t), \cdots s_K(t)])$, and $\mathrm{diag}(\bullet)$ denotes diagonal matrix. σ_k^2 represents the power of the kth incident signal. $\boldsymbol{A} = [\boldsymbol{a}_1, \boldsymbol{a}_2, \cdots, \boldsymbol{a}_K]$ is the steering vector matrix, and σ_{n}^2, $\boldsymbol{I}_M$ represent the noise power and $M \times M$ identity matrix, respectively.

The eigenvalue decomposition (EVD) of the covariance matrix $\boldsymbol{R_X}$ is

$$\boldsymbol{R_X} = \sum_{i=1}^{M} \lambda_i \boldsymbol{u}_i \boldsymbol{u}_i^{\mathrm{H}} \tag{8}$$

where λ_i is the real eigenvalue $\lambda_1 \ge \lambda_2 \cdots \ge \lambda_K > \lambda_{K+1} \cdots = \lambda_M = \sigma_{\mathrm{n}}^2$ and $\boldsymbol{u}_1, \boldsymbol{u}_2, \cdots \boldsymbol{u}_M$ are the corresponding orthonormal eigenvectors. Define two matrices $\boldsymbol{U}_S$ and $\boldsymbol{U}_N$ as

$$\boldsymbol{U}_S = [\boldsymbol{u}_1, \boldsymbol{u}_2, \cdots \boldsymbol{u}_K], \ \boldsymbol{U}_N = [\boldsymbol{u}_{K+1}, \cdots \boldsymbol{u}_M]. \tag{9}$$

$\boldsymbol{U}_S$ contains the eigenvectors corresponding to signal subspace and $\boldsymbol{U}_N$ the eigenvectors corresponding to noise subspace. The column vectors in $\boldsymbol{U}_S$ span the identical signal subspace as the column vectors in $\boldsymbol{A}$, then there must exist a unique nonsingular matrix $\boldsymbol{T}$

$$\boldsymbol{U}_S = \boldsymbol{A}\boldsymbol{T}. \tag{10}$$

Let $\boldsymbol{U}_{S1}$ and $\boldsymbol{U}_{S2}$ be the sub-matrices consisting of the first and the last $M-2$ rows of $\boldsymbol{U}_S$, respectively. Then

$$\boldsymbol{U}_{S1} = \boldsymbol{A}_1\boldsymbol{T}, \ \boldsymbol{U}_{S2} = \boldsymbol{A}_2\boldsymbol{T} \tag{11}$$

where $\boldsymbol{A}_1$ and $\boldsymbol{A}_2$ are the sub-matrices formed from $\boldsymbol{A}$ in the same way the $\boldsymbol{U}_{S1}$ and $\boldsymbol{U}_{S2}$ are formed from $\boldsymbol{U}_S$, then

$$\boldsymbol{A}_2 = \boldsymbol{A}_1\boldsymbol{\psi} \tag{12}$$

where $\boldsymbol{\psi}$ is a diagonal matrix described as below

$$\boldsymbol{\psi} = \mathrm{diag}\left([e^{j2\phi_1}, e^{j2\phi_2}, \cdots, e^{j2\phi_K}]\right). \tag{13}$$

It is obvious that the elements of $\boldsymbol{\psi}$ are only relevant to the directions of arrival. From (11) and (12), we can concluded that

$$\boldsymbol{U}_{S2} = \boldsymbol{A}_1\boldsymbol{\psi}\boldsymbol{T} = \boldsymbol{U}_{S1}\boldsymbol{T}^{-1}\boldsymbol{\psi}\boldsymbol{T} = \boldsymbol{U}_{S1}\boldsymbol{\Omega} \tag{14}$$

where $\boldsymbol{\Omega} = \boldsymbol{T}^{-1}\boldsymbol{\psi}\boldsymbol{T}$, that is $\boldsymbol{\Omega}\boldsymbol{T}^{-1} = \boldsymbol{T}^{-1}\boldsymbol{\psi}$. It can be seen that the diagonal elements of $\boldsymbol{\psi}$ are the eigenvalues of matrix $\boldsymbol{\Omega}$ and the column vectors of $\boldsymbol{T}^{-1}$ are the corresponding eigenvectors of $\boldsymbol{\Omega}$. Matrix $\boldsymbol{\Omega}$ could be calculated by using the TLS-ESPRIT algorithm as same in [4], then the estimation of elevation angle can be computed by determining the eigenvalues $e^{j2\phi_k}$ of $\boldsymbol{\Omega}$. Note that $\phi_k = 2\pi d\sin\theta_k/\lambda_k$, then

$$\hat{\theta}_k = \arcsin\left(\mathrm{angle}(e^{j2\phi_k})\frac{\lambda_k}{4\pi d}\right) \tag{15}$$

where $\text{angle}(\cdot)$ and $\arcsin(\cdot)$ represents the phase angle operation and arcsine operation, respectively.

A simple estimation method of polarization parameters will be introduced following.

Matrix A_1 has the following form

$$A_1 = \begin{bmatrix} p_{x1} & p_{x2} & \cdots & p_{xK} \\ p_{y1}e^{j\phi_1} & p_{y2}e^{j\phi_2} & \cdots & p_{yK}e^{j\phi_K} \\ \vdots & & \ddots & \vdots \\ p_{y1}e^{j(M-3)\phi_1} & p_{y2}e^{j(M-3)\phi_2} & \cdots & p_{yK}e^{j(M-3)\phi_K} \end{bmatrix}. \tag{16}$$

According to equation (16), let A_{1O} and A_{1E} be the sub-matrices of A_1 consisting of all the odd numbered rows and the even numbered rows, respectively. Then

$$A_{Div} = A_{1E}./A_{1O} = \begin{bmatrix} \frac{p_{y1}}{p_{x1}}e^{j\phi_1} & \frac{p_{y2}}{p_{x2}}e^{j\phi_2} & \cdots & \frac{p_{yK}}{p_{xK}}e^{j\phi_K} \\ \frac{p_{y1}}{p_{x1}}e^{j\phi_1} & \frac{p_{y2}}{p_{x2}}e^{j\phi_2} & & \frac{p_{yK}}{p_{xK}}e^{j\phi_K} \\ \vdots & \vdots & \ddots & \vdots \\ \frac{p_{y1}}{p_{x1}}e^{j\phi_1} & \frac{p_{y2}}{p_{x2}}e^{j\phi_2} & \cdots & \frac{p_{yK}}{p_{xK}}e^{j\phi_K} \end{bmatrix} \tag{17}$$

where $(./)$ represents corresponding elements division operation and A_{Div} is a $\left(\frac{M-2}{2}\right)\times K$ matrix with the same elements of each column. From equations (2) and(17), the absolute value and phase angle of the element of each column are

$$p_{1k} = \text{abs}\left(\frac{p_{yk}}{p_{xk}}e^{j\phi_k}\right) = \tan\gamma_k \cos\theta_k \text{ , } p_{2k} = \text{angle}\left(\frac{p_{yk}}{p_{xk}}e^{j\phi_k}\right) = \eta_k + \phi_k + \pi \text{ .} \tag{18}$$

After the EVD of $\boldsymbol{\Omega}$, the steering vector sub-matrix A_1 could be estimated as

$$\hat{A}_1 = U_{S1}T^{-1} = U_{S2}T^{-1}\psi^{-1} = \frac{1}{2}\left\{U_{S1}T^{-1} + U_{S2}T^{-1}\psi^{-1}\right\}. \tag{19}$$

Dividing all the odd numbered rows of $\hat{A}_1$ into the even numbered rows, that is $\hat{A}_{Div} = \hat{A}_{1O}./\hat{A}_{1E}$, then the estimation of polarization parameters can be obtained. Using the results of the eigenvalues of $\boldsymbol{\Omega}$ and equation (15), then the estimations of auxiliary polarization angle and polarization phase difference can be expressed as

$$\hat{\gamma}_k = \arctan\left(\frac{\hat{p}_{1k}}{\cos(\hat{\theta}_k)}\right), \hat{\eta}_k = \hat{p}_{2k} - \hat{\phi}_k - \pi. \tag{20}$$

In practice, in order to enhance the accuracy of polarization estimation, the $(M-2)/2$ estimates of each column of $\hat{A}_1$ are all used to calculate the mean value.

From the above derivation, it can be seen that the eigenvalues of $\boldsymbol{\Omega}$ are all used to complete the estimation of elevation angle, and the polarization estimation is achieved through the corresponding eigenvectors and the estimated elevation angle. Because of the eigenvalue and eigenvector is corresponding to each other, then the DOA and polarization parameter are paired automatically. Compared with the ESPRIT algorithm in [4], there is only once sub-array division, no need to pair the parameters, and less algorithm complexity and computation in this paper.

The Cramer-Rao Lower Bound (CRLB) is used to measure the accuracy of the proposed algorithm in the paper. In order to simplify the analysis, assume that the parameters need to be estimated are elevation angle and auxiliary polarization angle. There are K incident signals and $2K$ parameters need to be estimated, that is $\boldsymbol{v} = \{\theta_1, \theta_2, \cdots, \theta_K, \gamma_1, \gamma_2, \cdots, \gamma_K\}$. The Fisher Information Matrix (FIM) [14] can be described as

$$\boldsymbol{F} = \begin{bmatrix} \boldsymbol{F}_{\theta\theta} & \boldsymbol{F}_{\theta\gamma} \\ \boldsymbol{F}_{\gamma\theta} & \boldsymbol{F}_{\gamma\gamma} \end{bmatrix}. \tag{21}$$

The element of matrix $\boldsymbol{F}$ is given by

$$F_{lm} = N \cdot \text{tr}\left\{\boldsymbol{R}_X^{-1} \cdot \frac{\partial \boldsymbol{R}_X}{\partial v_l} \cdot \boldsymbol{R}_X^{-1} \cdot \frac{\partial \boldsymbol{R}_X}{\partial v_m}\right\} \tag{22}$$

where N is the number of sampling snapshots and $\text{tr}\{\}$ denotes the trace of the matrix. By using the operations of block matrix, the CRLB of $\boldsymbol{\theta}$ and $\boldsymbol{\gamma}$ is given by

$$\text{CRLB}(\boldsymbol{\theta}) = \left(\boldsymbol{F}_{\theta\theta} - \boldsymbol{F}_{\theta\gamma}\boldsymbol{F}_{\gamma\gamma}^{-1}\boldsymbol{F}_{\gamma\theta}\right)^{-1}, \text{CRLB}(\boldsymbol{\gamma}) = \left(\boldsymbol{F}_{\gamma\gamma} - \boldsymbol{F}_{\gamma\theta}\boldsymbol{F}_{\theta\theta}^{-1}\boldsymbol{F}_{\theta\gamma}\right)^{-1}. \tag{23}$$

After some algebraic operations, the elements of matrix $\boldsymbol{F}$ can be represented as

$$\boldsymbol{F}_{\theta\theta} = 2N\left(\boldsymbol{H}\boldsymbol{H}^{\mathrm{T}}\right) \odot \text{Re}\left\{\left(\boldsymbol{A}^{\mathrm{H}}\boldsymbol{R}_X^{-1}\boldsymbol{A}'_{\theta}\right) \odot \left(\boldsymbol{A}^{\mathrm{H}}\boldsymbol{R}_X^{-1}\boldsymbol{A}'_{\theta}\right)^{\mathrm{T}} + \left(\boldsymbol{A}^{\mathrm{H}}\boldsymbol{R}_X^{-1}\boldsymbol{A}\right) \odot \left(\boldsymbol{A}'^{\mathrm{H}}_{\theta}\boldsymbol{R}_X^{-1}\boldsymbol{A}'_{\theta}\right)^{\mathrm{T}}\right\}. \tag{24}$$

$$\boldsymbol{F}_{\gamma\gamma} = 2N\left(\boldsymbol{H}\boldsymbol{H}^{\mathrm{T}}\right) \odot \text{Re}\left\{\left(\boldsymbol{A}^{\mathrm{H}}\boldsymbol{R}_X^{-1}\boldsymbol{A}'_{\gamma}\right) \odot \left(\boldsymbol{A}^{\mathrm{H}}\boldsymbol{R}_X^{-1}\boldsymbol{A}'_{\gamma}\right)^{\mathrm{T}} + \left(\boldsymbol{A}^{\mathrm{H}}\boldsymbol{R}_X^{-1}\boldsymbol{A}\right) \odot \left(\boldsymbol{A}'^{\mathrm{H}}_{\gamma}\boldsymbol{R}_X^{-1}\boldsymbol{A}'_{\gamma}\right)^{\mathrm{T}}\right\}. \tag{25}$$

$$\boldsymbol{F}_{\theta\gamma} = 2N\left(\boldsymbol{H}\boldsymbol{H}^{\mathrm{T}}\right) \odot \text{Re}\left\{\left(\boldsymbol{A}^{\mathrm{H}}\boldsymbol{R}_X^{-1}\boldsymbol{A}'_{\gamma}\right) \odot \left(\boldsymbol{A}^{\mathrm{H}}\boldsymbol{R}_X^{-1}\boldsymbol{A}'_{\theta}\right)^{\mathrm{T}} + \left(\boldsymbol{A}^{\mathrm{H}}\boldsymbol{R}_X^{-1}\boldsymbol{A}\right) \odot \left(\boldsymbol{A}'^{\mathrm{H}}_{\gamma}\boldsymbol{R}_X^{-1}\boldsymbol{A}'_{\theta}\right)^{\mathrm{T}}\right\}. \tag{26}$$

$$\boldsymbol{F}_{\gamma\theta} = \boldsymbol{F}_{\theta\gamma}^{\mathrm{T}}. \tag{27}$$

where $\boldsymbol{H} = [\sigma_1^2\ \sigma_2^2 \cdots \sigma_K^2]^{\mathrm{T}}$, $\boldsymbol{A}'_{\theta} = [\boldsymbol{a}'_1, \boldsymbol{a}'_2, \cdots, \boldsymbol{a}'_K]$ represents the partial derivative matrix of A and $A'_{\theta} = \frac{\partial A}{\partial \theta}$, $A'_{\gamma} = \frac{\partial A}{\partial \gamma}$, The elements of A'_{θ} and A'_{γ} are given by

$$\boldsymbol{a}'_{\theta} = [0, \frac{j\pi(\cos\theta)^2 - \sin\theta}{\cos\theta}, j2\pi\cos\theta, \cdots, j(M-2)\pi\cos\theta, \frac{j(M-1)\pi(\cos\theta)^2 - \sin\theta}{\cos\theta}]^{\mathrm{T}}. \tag{28}$$

$$\boldsymbol{a}'_{\gamma} = \left[\sin\gamma, j\cos\theta\cos\gamma e^{j\phi}, \sin\gamma e^{j2\phi}, \cdots, j\cos\theta\cos\gamma e^{j(M-1)\phi}\right]^{\mathrm{T}}. \tag{29}$$

4. SIMULATION ANALYSIS

In the first scenario, a 12-element uniform linear array of non-collocated vector sensor and a six-element uniform linear array of two-component collocated vector sensor are chosen to ensure the same 12 components for different array. The inter-element spacing is set to be $d = \lambda/2$ and the sampling snapshots is $N = 200$. A narrowband signal is considered and the DOA and polarization parameters are $(\theta_1, \varphi_1) = (25^\circ, 90^\circ)$ and $(\gamma_1, \eta_1) = (60^\circ, 90^\circ)$, respectively. Fig.3 and Fig.4 show a comparison between the performances of the proposed algorithm and CRLB. The Mean-Square Error (MSE) of θ and γ versus signal to noise ratio (SNR) are shown in Fig.3 and Fig.4, respectively.

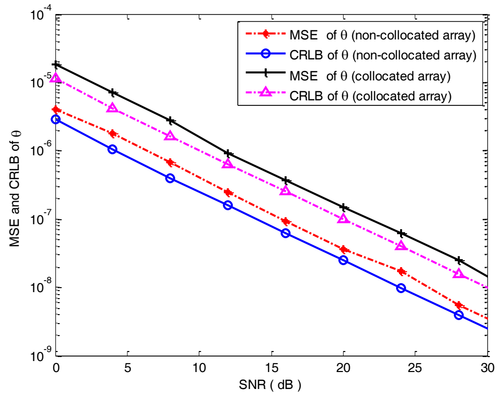

Fig.3 The comparison between MSE and CRLB of θ

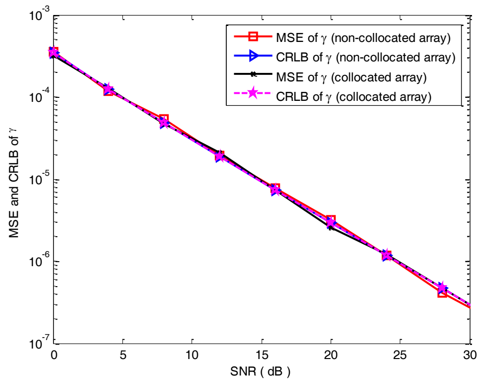

Fig.4 The comparison between MSE and CRLB of γ

For the two arrays with same components, the non-collocated array has a lower MSE and CRLB of θ than the collocated array in Fig.3. By distributing spatially the components of collocated sensor, the non-collocated vector sensor array can provide more freedom degrees and augment array aperture, so it can obtain more spatial information of incident signals. Thus, the accuracy of DOA estimation is improved. In Fig.4, different array forms have almost no effect on the accuracy of the polarization estimation and the MSE of γ is close to CRLB. That is because the equal number of components ensures the identical response to the polarization information of incident signals.

In the second scenario, a 12-element linear array of non-collocated vector sensor and also a 12-element linear array of two-component collocated vector sensor are chosen to satisfy the identical array aperture for different array. The same incident signal parameters and inter-element spacing with the first scenario are considered. The MSE of θ and γ versus SNR under different array forms are shown in Fig.5 and Fig.6, respectively.

For the two arrays with same array aperture, the collocated array has a slightly lower MSE of θ than the non-collocated array in Fig.5. The extra component of each collocated sensor can receive a little more spatial information compared with the single component in non-collocated array, but it has a slight effect on the accuracy of DOA estimation.

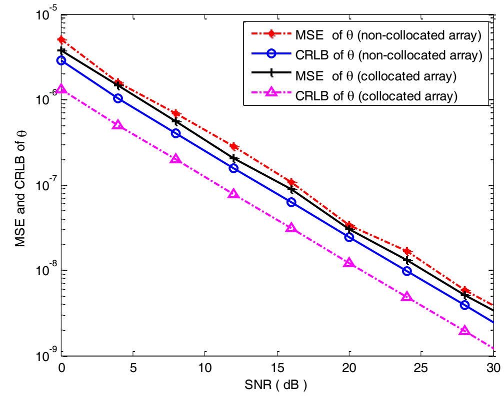

Fig.5 The comparison between MSE and CRLB of θ

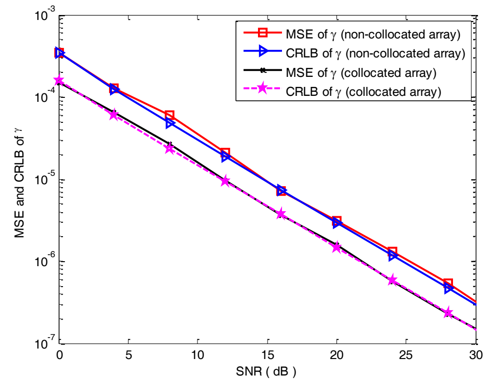

Fig.6 The comparison between MSE and CRLB of γ

Due to the same array aperture, the ability to obtain spatial information is not much difference between the two arrays. So the performance of DOA estimation is similar but the number of components is reduced by half in non-collocated array. In Fig.6, the collocated array has a more effective estimation performance of γ than the non-collocated array. That is because double components in collocated array significantly increase the ability to achieve polarization information and the accuracy of polarization estimation is improved. However, more components also bring more hardware cost of antenna implementation and algorithm complexity.

5. CONCLUSION

An ESPRIT-based method using a spatially non-collocated vector sensor array is derived to achieve the DOA and polarization estimation in this paper. Simulation results indicate that the accuracy of DOA estimation is mostly determined by the array aperture and the polarization estimation much depends on the number of components. Furthermore, the number of components and the hardware cost of antenna implementation in non-collocated array is reduced by half but the performance of DOA estimation is close to that in collocated array, so the non-collocated array has more potential advantages.

REFERENCES

[1] X. Zhang, Y. Shi, and D. Xu. "Novel blind joint direction of arrival and polarization estimation for polarization-sensitive uniform circular array," *Progress In Electromagnetics Research*, pp. 19-37, 2008.

[2] K.T. Wong. "Direction finding/polarization estimation-dipole and/or loop triad (s)," *IEEE Trans. Aerospace and Electronic Systems*, Vol. 37, no. 2, pp. 679-684, 2001.

[3] K.T. Wong, and M.D. Zoltowski, "Uni-vector sensor esprit for multisource azimuth, elevation, and polarization estimation," *IEEE Trans. Antennas and Propagation*, Vol. 45, pp.1467 - 1474, 1997.

[4] J. Li, and T. Compton. "Angle and polarization estimation using ESPRIT with a polarization sensitive array," *IEEE Trans. Antennas and Propagation*, Vol. 39, no. 9, pp. 1376-1383, 1991.

[5] K.T. Wong, and M.D. Zoltowski. "Closed-form direction finding and polarization estimation with arbitrarily spaced electromagnetic vector-sensors at unknown locations," *IEEE Trans. Antennas and Propagation*, Vol. 48, no. 5, pp. 671-681,2000.

[6] A. Nehorai, and C. Ho. "Minimum-noise-variance beamformer with an electromagnetic vector sensor," *IEEE Trans. Signal Process*, Vol. 47, no. 3, pp. 601-618, 1999.

[7] Y.G Xu, T. Liu, and Z.W. Liu. "Output SINR of MV beamformer with one EM vector sensor of and magnetic noise power," *in 7th International Conference on Signal Processing*, pp. 419-422, 2004.

[8] S. Durrani, and E. Bialkowski. "Effect of mutual coupling on the interference rejection capabilities of linear and circular arrays in CDMA systems," *IEEE Trans. Antennas and Propagation*, Vol. 52, no. 4, pp. 1130-1134, 2004.

[9] C. See, and A. Nehorai. "Source localization with distributed electromagnetic component sensor array processing," *Proc. of the 7th International Symposium on Signal Processing and Its Applications*, 2003, pp.177-180.

[10] K.T. Wong, and X. Yuan. "Vector cross-product direction-finding with an electromagnetic vector-sensor of six orthogonally oriented but spatially noncollocating dipoles/loops," *IEEE Trans. Signal Process*, Vol. 59, no. 1, pp. 160-171, 2011.

[11] X. Yuan. "Cramer-Rao bound of the direction-of-arrival estimation using a spatially spread electromagnetic vector-sensor," *IEEE International Conf. Statistical Signal Processing Workshop*, 2011, pp. 1-4.

[12] J. Li. "Direction and polarization estimation using arrays with small loops and short dipoles," *IEEE Trans. Antennas and Propagation*, Vol. 41, no. 3, pp. 379-384, 1993.

[13] Z.H. Xu, and Z.Y. Xiong. "A Novel Alternate Polarization Array and Its Filtering Performance," *2011 IEEE CIE International Conference on Radar*, Chengdu, pp. 1890-1892, 2011.

[14] P. Stoica, and E.G Larsson. "The stochastic CRB for array processing: a textbook derivation," *Signal Processing Letters*, Vol. 8, no.5, pp. 148-150, 2001.